8-2020

Gain-of-function variants and overexpression of RUNX2 in patients with nonsyndromic midline craniosynostosis

Araceli Cuellar
University of California Davis School of Medicine

Krithi Bala
University of California Davis School of Medicine

Lorena Di Pietro
Università Cattolica del Sacro Cuore

Marta Barba
Università Cattolica del Sacro Cuore

Garima Yagnik
University of California Davis School of Medicine

See next page for additional authors

Gain-of-function variants and overexpression of RUNX2 in patients with nonsyndromic midline craniosynostosis

Abstract

Craniosynostosis (CS), the premature fusion of one or more cranial sutures, is a relatively common congenital anomaly, occurring in 3–5 per 10,000 live births. Nonsyndromic CS (NCS) accounts for up to 80% of all CS cases, yet the genetic factors contributing to the disorder remain largely unknown. The *RUNX2* gene, encoding a transcription factor critical for bone and skull development, is a well known CS candidate gene, as copy number variations of this gene locus have been found in patients with syndromic craniosynostosis. In the present study, we aimed to characterize *RUNX2* to better understand its role in the genetic etiology and in the molecular mechanisms underlying midline suture ossification in NCS. We report four nonsynonymous variants, one intronic variant and one 18 bp in-frame deletion in *RUNX2* not found in our study control population. Significant difference in allele frequency (AF) for the deletion variant *RUNX2* p.Ala84-Ala89del (ClinVar 257,095; dbSNP rs11498192) was observed in our sagittal NCS cohort when compared to the general population ($P = 1.28 \times 10-6$), suggesting a possible role in the etiology of NCS. Dual-luciferase assays showed that three of four tested *RUNX2* variants conferred a gain-of-function effect on RUNX2, further suggesting their putative pathogenicity in the tested NCS cases. Downregulation of *RUNX2* expression was observed in prematurely ossified midline sutures. Metopic sites showed significant downregulation of promoter 1-specific isoforms compared to sagittal sites. Suture-derived mesenchymal stromal cells showed an increased expression of *RUNX2* over matched unfused suture derived cells. This demonstrates that *RUNX2*, and particularly the distal promoter 1-isoform group, are overexpressed in the osteogenic precursors within the pathological suture sites.

Keywords

Nonsyndromic craniosynostosis, Craniofacial, Birth defect, RUNX2, Mesenchymal stromal cells, Osteogenesis

Disciplines

Congenital, Hereditary, and Neonatal Diseases and Abnormalities | Genomics | Medical Genetics

Comments

This article is published as Cuellar, Araceli, Krithi Bala, Lorena Di Pietro, Marta Barba, Garima Yagnik, Jia Lie Liu, Christina Stevens et al. "Gain-of-function variants and overexpression of RUNX2 in patients with nonsyndromic midline craniosynostosis." *Bone* 137 (2020): 115395. DOI: 10.1016/j.bone.2020.115395.

Authors

Araceli Cuellar, Krithi Bala, Lorena Di Pietro, Marta Barba, Garima Yagnik, Jia Lie Liu, Christina Stevens, David J. Hur, Roxann G. Ingersoll, Cristina M. Justice, Hicham Drissi, Jinoh Kim, Wanda Lattanzi, and Simeon A. Boyadjiev

Bone 137 (2020) 115395

Contents lists available at ScienceDirect

Bone

journal homepage: www.elsevier.com/locate/bone

Full Length Article

Gain-of-function variants and overexpression of *RUNX2* in patients with nonsyndromic midline craniosynostosis

Araceli Cuellar[a,1], Krithi Bala[a,1], Lorena Di Pietro[b,1], Marta Barba[b,c,1], Garima Yagnik[a], Jia Lie Liu[a], Christina Stevens[a], David J. Hur[d], Roxann G. Ingersoll[e], Cristina M. Justice[f], Hicham Drissi[g], Jinoh Kim[h], Wanda Lattanzi[b,c,*], Simeon A. Boyadjiev[a,*]

[a] Department of Pediatrics, University of California Davis School of Medicine, Sacramento, CA, USA
[b] Dipartimento Scienze della Vita e Sanità Pubblica, Sezione di Biologia Applicata, Università Cattolica del Sacro Cuore, Rome, Italy
[c] Fondazione Policlinico Universitario A. Gemelli IRCCS, Rome, Italy
[d] Section of Cardiovascular Medicine, Department of Internal Medicine, Yale School of Medicine, New Haven, CT, USA
[e] Mc-Kusick-Nathans Institute of Genetic Medicine, Johns Hopkins, Baltimore, MD, USA
[f] Genometrics Section, Computational and Statistical Genomics Branch, Division of Intramural Research, NHGRI, NIH, Baltimore, MD, USA
[g] Department of Orthopaedics, Emory University School of Medicine, Atlanta, GA, USA
[h] Department of Biological Sciences, College of Veterinary Medicine, Iowa State University, IA, USA

ARTICLE INFO

Keywords:
Nonsyndromic craniosynostosis
Craniofacial
Birth defect
RUNX2
Mesenchymal stromal cells
Osteogenesis

ABSTRACT

Craniosynostosis (CS), the premature fusion of one or more cranial sutures, is a relatively common congenital anomaly, occurring in 3–5 per 10,000 live births. Nonsyndromic CS (NCS) accounts for up to 80% of all CS cases, yet the genetic factors contributing to the disorder remain largely unknown. The *RUNX2* gene, encoding a transcription factor critical for bone and skull development, is a well known CS candidate gene, as copy number variations of this gene locus have been found in patients with syndromic craniosynostosis. In the present study, we aimed to characterize *RUNX2* to better understand its role in the genetic etiology and in the molecular mechanisms underlying midline suture ossification in NCS. We report four nonsynonymous variants, one intronic variant and one 18 bp in-frame deletion in *RUNX2* not found in our study control population. Significant difference in allele frequency (AF) for the deletion variant *RUNX2* p.Ala84-Ala89del (ClinVar 257,095; dbSNP rs11498192) was observed in our sagittal NCS cohort when compared to the general population ($P = 1.28 \times 10^{-6}$), suggesting a possible role in the etiology of NCS. Dual-luciferase assays showed that three of four tested *RUNX2* variants conferred a gain-of-function effect on RUNX2, further suggesting their putative pathogenicity in the tested NCS cases. Downregulation of *RUNX2* expression was observed in prematurely ossified midline sutures. Metopic sites showed significant downregulation of promoter 1-specific isoforms compared to sagittal sites. Suture-derived mesenchymal stromal cells showed an increased expression of *RUNX2* over matched unfused suture derived cells. This demonstrates that *RUNX2*, and particularly the distal promoter 1-isoform group, are overexpressed in the osteogenic precursors within the pathological suture sites.

1. Introduction

The final shape of the cranium is achieved through a complex interaction of multiple skull osseous elements, dura mater, and the brain. Bands of dense fibrous tissue connecting the flat bones of the skull, known as sutures, provide the plasticity needed for non-traumatic passage through the birth canal and for the accommodation of the rapidly growing brain in the first years of life. Premature fusion of one or more cranial sutures results in craniosynostosis (CS), one of the most common craniofacial anomalies that manifests with an abnormal skull shape. CS is a heterogeneous condition with regards to both etiology and pathogenesis, and its reported incidence varies from 3 to 5 per 10,000 live births. Mendelian mutations account for approximately 20–25% of all CS cases and are described as syndromic as they are usually associated with additional anomalies and/or developmental delays [1,2]. Mutations in one of at least ten genes (*EFNB1, FGFR1-3, MSX2, POR, RAB23, TCF12, ERF,* and *TWIST1*) are associated with most common types of syndromic CS (Apert, Crouzon, Jackson-Weiss,

* Corresponding authors.
E-mail addresses: wanda.lattanzi@unicatt.it (W. Lattanzi), sboyd@ucdavis.edu (S.A. Boyadjiev).
[1] AC, KB, LDP and MB contributed equally.

https://doi.org/10.1016/j.bone.2020.115395
Received 14 January 2020; Received in revised form 23 April 2020; Accepted 26 April 2020
Available online 30 April 2020
8756-3282/ Published by Elsevier Inc.

Pfeiffer, Saethre-Chotzen, Beare-Stevenson and Muenke syndromes) [3–7]. Nonsyndromic CS (NCS), usually affecting single sutures in an otherwise normal skull, accounts for up to 80% of all CS cases, yet the genetic factors contributing to the disorder remain largely unknown. To date, single gene mutations in only a few genes, namely *FGFR3*, *TWIST1*, *EFNB1*, and *TCF12* [8–12] have been found to cause single suture CS, though usually in association with additional syndromic features.

It has been shown that the development and maintenance of cranial sutures is controlled by several regulatory factors including those involved in the BMP/ TGF-β, FGF, hedgehog (HH), eph-ephrin, and Wnt signaling pathways. These pathways converge on the same downstream effector Runt-related transcription factor 2 (*RUNX2*) [13], a strong candidate gene in CS. Copy number variations in the *RUNX2* locus have been found in CS patients. Specifically, a duplication of the *RUNX2* locus on 6p21.1 was described in patients with metopic CS and minor additional features [14,15]. *RUNX2* triplication [16] and quadruplication [17] were found in patients with more complex syndromic phenotypes, including combined coronal and sagittal synostosis [16] or pan-craniosynostosis [17], respectively. This observation clearly suggests a dosage effect of *RUNX2* mutations, with midline (metopic and sagittal) sutures appearing to be the primary target sites of the dysmorphic insult.

On the other hand, haploinsuficiency of *RUNX2* due to loss-of-function (LOF) mutations causes cleidocranial dysplasia, characterized by hypo-ossification in membranous bones (i.e. calvarial bones and clavicles), with failure of cranial suture fusion, in addition to other anomalies [18].

These clinical correlates confirm the key role of this gene in skull development.

RUNX2 is an osteoblast-specific transcription factor and functions as a regulator of osteoblast differentiation [19,20]. RUNX2 is necessary in the early stages of osteogenic differentiation (mesenchymal stromal cells commitment and differentiation into pre-osteoblasts). During the later stages (differentiation of pre-osteoblasts into mature osteoblasts and then osteocytes), RUNX2 levels decrease [21–23]. *RUNX2* encodes 12 alternatively spliced transcript variants, of which 7 are protein-coding variants, 3 are destined to nonsense mediated decay, and 2 are classified as processed transcripts (source: https://www.ensembl.org/). *RUNX2* transcripts are transcribed from two different promoters, a distal promoter (Promoter 1, P1) and a proximal one (Promoter 2, P2) (Fig. 1) P1 and P2 are separated by an exon and a large intron, and the proteins derived from the the two promoters differ at the N-terminus for 19 amino acids [24,25]. In mice, P1 is activated during osteogenesis and is required for bone formation, while P2 is expressed in both osseous and non-osseous mesenchyme, thus it is not exclusively linked to osteogenesis [26,27]. Changes in *RUNX2* expression (either gain- or loss-of-function) significantly impact osteoblastic differentiation and skull development. This sort of site-specific effect may be due to the chronology of skull morphogenesis and ossification, metopic suture being the very first to complete the fusion during early perinatal stages. Hence, the effect of *RUNX2* mutations on skeletal development may depend on the specific stage impaired by the aberrant RUNX2 dosage, which is involved in regulating the balance of osteogenic proliferation/ differentiation in suture tissues [6].

In order to study the possible contribution of *RUNX2* to NCS etiopathogenesis, we have characterized this gene in a cohort of patients with sagittal and metopic NCS. In particular, we searched for coding sequence variations occurring in patients and analyzed the differential expression of the transcript variants bearing either of the two alternative promoters in patients suture tissues and in cells derived thereof.

2. Materials and methods

2.1. Patients and biospecimens

Probands affected by sagittal NCS (sNCS) and metopic NCS (mNCS) were selected for this study. Probands were recruited from multiple institutions collaborating within the International Craniosynostosis Consortium (https://health.ucdavis.edu/pediatrics/boyd-genetics-lab/index.html). The evaluation of probands was based on clinical examination by a clinical geneticist or a referring surgeon and/or review of the medical documentation, photographs, and existing CT scans. Paired calvarial tissue samples, from the physiological patent suture (termed unfused) and from the prematurely fused suture were provided by the Pediatric Neurosurgery Unit of the Fondazione Policlinico Universitario “A. Gemelli” – IRCCS (Rome). The tissue samples were processed for RNA extraction and cell isolation as described below. The study was approved by the Institutional Review Board of the University of California Davis and the Ethical Committee of the Università Cattolica del Sacro Cuore and was conducted in accordance with the institutional guidelines for human subject research. Informed consents were obtained from all study participants prior to review of medical documentation, clinical examinations and sample collection.

2.2. PCR and sequencing

DNA was extracted from blood, saliva or mouthwash according to the manufacturer's protocol using the Gentra Puregene Blood Kit (QIAGEN). Genomic DNA from 50 unrelated and unaffected individuals was used for control frequency analysis. PCR primers were selected from the published RefSeq sequence of RUNX2 gene using the Gene Runner software (Hastings Software, Inc.). At least 100 bases of flanking intronic sequence was included for each exon and the 5′- and 3′-untranslated regions (UTR) of the candidate gene. PCR products were purified using ExoSap-IT (Affymetrix). Electropherograms were analyzed with the Vector NTI ContigExpress software by two independent investigators. All observed variants were confirmed by independent PCR and secondary sequencing using the reverse primer. For the variant RUNX2 p.Ala84-Ala89del, independent PCR products were analyzed by gel electrophoresis using a 2% agarose gel. RFLP analysis was also performed for some variants to confirm the findings from their respective sequencing results.

2.3. Bioinformatic and computational analysis

SNPs were considered novel if not present in the following databases: NCBI dbSNP, ExAC, or 1000Genomes. Conservation across multiple species in amino acid residues altered by mutations was done using ClustalW software. Possible harmful effect of the SNPs were determined by SIFT and PPH prediction software (SIFT, Fred Hutchinson Cancer Research Center, Seattle, web software, http://blocks.fhcrc.org/sift/SIFT.html; PPH, Bork Group & Sunyaev Lab, Harvard, web software, http://genetics.bwh.harvard.edu/pph). All noncoding variants were analyzed for predicted alteration of promoter and/or transcriptional factor binding sites with the MatInspector and TESS programs http://www.genomatix.de/cgi-bin/eldorado/main.pl and http://www.cbil.upenn.edu/tess/, respectively [28,29]. The rVISTA program (https://rvista.dcode.org/) was used to analyze conservation of these variants across species in an effort to reduce false positive findings [30]. All variations were also analyzed for cryptic splice site formation using a splice site prediction program (http://www.fruitfly.org/seq_tools/splice.html) [31]. This was carried out using a method analogous to promoter analysis with 50 bases flanking each side, and with the minimum score for both the 5′ and 3′ splice sites set at 0.8. Branch A site analysis was carried out using Gene Runner software (Hastings Software, Inc.) for variations 5′ of the acceptor splice sites. We compared the consensus sequence for the branch A site against each allele,

flanked by 10 bases on each side. Variations located at the 3′ of each gene were analyzed for possible alteration of the poly A site.

2.4. Cell culture

Human calvarial osteoblasts (HCO) were obtained from ScienCell Research Laboratories (Carlsbad, CA, USA) and cultured in DMEM (Gibco) containing 10% FBS (Atlanta Biologicals) and 1% penicillin-streptomycin (Gibco). HCO cells were used for luciferase assay (see further sections). Calvarium-derived mesenchymal stromal cells (CMSC) were isolated in primary explant tissue culture from open and fused sutures of 33 NCS patients (16 metopic and 17 sagittal), and cultured in DMEM (Aurogene, Rome, Italy) containing 10% FBS (Aurogene), 1% L-glutamine (Euroclone, Milan, Italy) and 1% penicillin-streptomycin (Euroclone), according to standardized methods as described [32]. Cells were characterized by cytometry and CMSC phenotype was confirmed (data not shown) [33]. Confluent CMSC culture were detached by trypsin digestion and collected for RNA isolation. All CMSC were used between the third (P3) and fourth (P4) passage of culture.

2.5. Vector construction

Expression vectors for all *RUNX2* variants were constructed using pCMV6 and pGL-3 was used as the reporter vector. The expression vector construct was made by amplification of human RUNX2 cDNA from OriGene clone (RC212884), digestion with restriction enzymes Sgfl and Mlul (New England Biolabs) and ligation into pCMV6. Mutation variants were introduced via QuikChange Lighting Site-Directed Mutagenesis Kit (Stratagene) according to manufacturer's instructions, re-ligated into pCMV6 and transformed into *E. coli*. *E. coli* was plated on agar plates with ampicillin and surviving colonies were purified via Qiagen Midi-Prep kits. Constructs were sequenced to confirm the presence of each variant.

2.6. Dual-luciferase assay

HCO cells were incubated in 96-well plates at a density of 5×10^3/well before transfection. After growing for 24 h, cells were transfected using Lipofectamine 3000 (Invitrogen) according to manufacturer's instructions. Cells were co-transfected with an empty pCMV6 or a RUNX2 variant expression vector and a firefly luciferase reporter construct containing six runx2 DNA-binding elements (*pOSE2*-Luc) [34]. *Renilla* vector was used as an internal control. Luminescence was produced by the Dual-Luciferase Reporter Assay System (Promega) according to manufacturer's protocol and measured with a Turner BioSystems™ 20/20 Luminometer. All transfections trials were performed independently 6 times in triplicate. Experimental data was analyzed by one-way analysis of variance and $P < 0.05$ was considered significantly different.

2.7. Suture tissue processing

Calvarial tissue specimens obtained from 19 patients (10 metopic, 9 sagittal) were immediately frozen upon collection and cryopreserved until RNA extraction. The snap-frozen calvarial tissue specimens were grinded using a mortar and pestle, before RNA isolation.

2.8. RNA isolation

Suture tissue homogenates and CMSC were lysate using TRIzol Reagent (Invitrogen, Carlsbad, CA, USA) [33]. RNA was then isolated using silica membrane spin columns (Direct-zol RNA Kit, Zymo Research, Irvine, CA, USA), according to the manufacturer's protocol. The yield and quality of RNA were determined using the DU 800 Spectrophotometer (Beckman Coulter, Brea, CA, USA).

2.9. RT-qPCR

The expression of *RUNX2* was analyzed in suture tissues and cells using RT-qPCR, according to standardized methods described elsewhere [32]. To also consider the alternatively spliced variants along with the multiple promoters of the gene, different sequence-specific oligonucleotide primer sets were designed to amplify either the total mRNA content or the alternative transcripts (see Supplemental Table 1). 500 ng of total RNA were used as template for cDNA synthesis (GoScript™ Reverse Transcription System, Promega Corporation, Madison, WI, USA) and amplified by RT-qPCR using GoTaq® qPCR Master Mix (Promega Corporation). All RT-qPCR reactions were performed in triplicate, and the amplified signals from *RUNX2* were normalized to that of the housekeeping gene, *β-ACTIN* (*ACTB),* and the fold change (FC) was calculated using the ΔΔCt method using the unfused suture tissue as control in the comparison [35]. Data were analyzed using GraphPad Prism software version 6.0. Results are presented as mean FC ± SD. Statistical differences between groups were analyzed using the unpaired Student's *t*-test. All statistics were two-tailed and the level of significance was set at $p < 0.05$.

3. Results

3.1. RUNX2 variant screening

We initially sequenced the entire coding sequence of *RUNX2* in a discovery cohort composed of 20 sNCS probands. Two nonsynonymous familial SNPs - c.751C > T (R251C) and c.1489G > A (G497S) - were identified in the discovery cohort and were not present in 100 control chromosomes. Based on these findings, sequencing was conducted on an additional cohort of 191 sNCS patients and identified a total of six variants in *RUNX2*, five of which were in the coding regions of the gene (Table 1). The intronic IVS6 + 46 G > A variant was excluded from further analyses. Bioinformatic analyses were conducted using both SIFT and PPH prediction programs and all variants in the coding regions of the gene were predicted to be damaging. Based on these predictions all 5 variants were used for further functional studies; however, c. 1361 A > G Y454C was removed due to technical difficulties. These variants were previously reported in known databases, such as HapMap, NCBI or 1000Genomes.

3.2. Incidence validation of RUNX2 p.Ala84-Ala89del variant

Of the identified *RUNX2* variants, RUNX2 p.Ala84-Ala89del variant was present as heterozygous in 30% of sequenced sNCS probands. This inframe deletion results in the removal of 6 Alanines from a poly-Ala stretch in the glutamine-alanine (QA) domain (17Ala > 11Ala) and a similar deletion was recently suggested as pathogenic for CCD [36]. To validate the variant frequency among probands with sNCS and mNCS, we screened an additional 127 sNCS probands, as well as a cohort of 191 mNCS probands by gel electrophoresis in order to compare the RUNX2 p.Ala84-Ala89del variant frequency between the sagittal and metopic NCS subtypes. A comparison of allele frequency (AF) between the sNCS and mNCS cohorts versus the general population was performed. Within our combined NCS cohort of 461 probands (922 alleles) scored for RUNX2 p.Ala84-Ala89del, a total of 110 alleles were identified (11.9%) (AF = 0.119, based on Hardy-Wainberg) [37]. Using Pearson's Chi-square test, this difference in frequency compared to that of the general population (0.0813; gnomAD Database) was significant ($P = 2.83 \times 10^{-5}$). When comparing each NCS subtype to the general population, the AF of RUNX2 p.Ala84-Ala89del in the sNCS cohort (AF = 0.155) was significant different ($P = 1.28 \times 10^{-6}$). No significant difference in AF between the mNCS cohort (AF = 0.068) and the general population was observed ($P = 0.193$), demonstrating that the sagittal suture drove the significant difference observed in our NCS cohort. Analyzing between NCS subtypes, the AF of RUNX2 p.Ala84-

Ala89del between the sNCS cohort and the mNCS cohort were significantly different ($P = 3.08 \times 10^{-4}$).

3.3. Functional assay of RUNX2 mutations

We performed a dual-luciferase assay in order to determine the potential functional effect of the four *RUNX2* variants. The reporter vector for all assays was created by cloning the known RUNX2 binding element OSE2 [34] upstream of the minimal promoter for firefly luciferase (*pOSE2*-Luc). We used the following expression vectors: an empty vector (pCMV6), a wild-type RUNX2 cDNA clone (WT) and four vectors mutagenized for each of the variants R251C, D334N, G511S, and p.Ala84-Ala89del. We were not able to create an expression vector for the Y454C variant. Additionally, a known LOF M175R variant causing CCD [38] was used as a control. Each assay was carried out by transfecting pOSE2-Luc and one of the RUNX2 expression vectors into HCO cells. R251C, D334N, and p.Ala84-Ala89del show statistically significant increases in luminescence over WT (Fig. 2) with fold increases of 1.5, 1.3, and 2.9 respectively. As expected, the empty vector pCMV6 showed minimal luminescence and luminescence with G511S and M175R was lower as compared to WT, indicating possible LOF functuality.

3.4. RUNX2 isoform analysis

We then mapped the identified sequence variants in the alternative transcripts deriving from P1 and P2 promoters of the *RUNX2* gene. Fig. 1 shows the position of the 5 *RUNX2* variants identified within the coding sequence of the gene (see Table 1 for details of gene variants): rs11498192 (p.Ala84-Ala89del), rs11498200 (R251C) and rs373752642 (D334N) map in regions shared by all the coding isoforms, whereas rs1216479084 (Y454C) and rs11498198 (G511S) map in an exon that is skipped in the ENST00000576263.5 splice variant (Fig. 1). Four of the variants (R251C, D334N, Y454C and G511S) do not appear to fall within functional/binding domains of the RUNX2 protein, while the RUNX2 p.Ala84-Ala89del variant is within the QA domain of the gene. The alternative promoters of the human *RUNX2* are know to drive chronologically phased transcriptional patterns during skull morphogenesis [26]. Therefore, to assess the contribution of the different transcript isoforms in the ossification patterns of metopic and sagittal sutures of NCS patients, we analyzed *RUNX2* expression in matched fused versus open (unfused) suture tissue samples, and in matched calvarial mesenchymal stromal cells (CMSC) derived from fused versus open sutures of patients with either sNCS or mNCS.

RUNX2 total expression was significantly reduced in both mNCS and sNCS fused suture tissues compared to patient-matched unfused sites (Fig. 3A). The expression of P1-derived isoforms was significantly down-regulated in mNCS fused sutures, while the P2-derived isoforms did not show statistically significant differences between fused and unfused tissues of both mNCS and sNCS (Fig. 3A). In sNCS patients, P1-derived *RUNX2* isoforms were significantly overexpressed in CMSC from fused sutures, when compared with those from the patient-matched open sutures (Fig. 3B). The total gene expression and that of the P2-derived isoforms did not display statistically significant differences between the two groups in sNCS (Fig. 3B). Conversely, in mNCS patients, both total and P2 isoform expression levels were significantly higher in CMSC from fused sutures compared with those from the matched open sutures (Fig. 3B). P1-derived isoform expression levels showed an increasing trend in CMSC from fused sutures over unfused ones in mNCS, though they did not reach a statistically significant difference (Fig. 3B).

We analyzed *RUNX2* expression levels in fused suture tissues and in CMSC comparatively between mNCS versus sNCS groups. We observed that *RUNX2* expression of both total mRNA and of the P1-derived isoforms were significantly downregulated in mNCS fused sutures when compared to sNCS fused sutures (Fig. 4). In suture tissues and CMSC, P2-derived isoforms expression did not significantly change within the two patient groups (Fig. 4). No significant change in *RUNX2* total expression was observed in fused suture-derived CMSC between sNCS and mNCS (Fig. 4). Finally, we have validated the expression of *RUNX2* in an indenpendent set of samples from unrelated patients with sagittal CS. This time unmatched unfused sagittal suture tissues and fused sagittal suture tissues from different individuals were comparatively analyzed in different permutations. Our analysis highlighted that both total and P1-derived *RUNX2* isoform levels decrease in fused sagittal compared with unfused sagittal sites, while the P2-derived isoforms did not show statistically significant differences between the two groups (Fig. 5).

4. Discussion

The *RUNX2* gene encodes the master osteogenic transcription factor, playing a crucial role in osteoblastic differentiation [22] and in craniofacial development, specifically affecting membranous ossification [39]. *RUNX2* excessive dosage is known to reproducibly cause syndromic craniosynostosis, mostly affecting the metopic and sagittal sutures [14,16,17,40]. Additionally, murine models with early *RUNX2* transgenic expression in mesenchymal cells display premature ossification of skull sutures resulting in craniosynostosis, suggesting that RUNX2 is a key player in driving the early stages of mesenchymal cells differentiation into osteoblasts, and leading to intramembranous bone formation during embryogenesis [41]. In this study, sequencing of *RUNX2* in NCS patients identified four nonsynonymous variants, one intronic variant and one 18 bp deletion. All *RUNX2* variants were significantly enriched in our study cohort ($P \leq 0.05$), except for G511S and p.Ala84-Ala89del in mNCS (Table 1).

Functional studies of the *RUNX2* variants based on dual-luciferase assays showed gain-of-function (GOF) effects from three of the four tested variants. In the RUNX2 isoform ENST00000647337.2 (NM_001278478; GRCh38), the glutamine-alanine repeats (QA) transactivation domain spans amino acids 49–89, and the highly conserved Runt-homologous DNA-binding domain spans amino acids 101–229. Four coding variants (R251C, D334N, Y454C and G511S) are outside of both the glutamine-alanine repeats (QA) transactivation domain and the highly conserved Runt- homologous DNA binding domain, and are not expected to affect other functional domains. The RUNX2 p.Ala84-Ala89del removes 6 alanines at amino acids 73–78 of the QA domain, which is has been shown to serve as an activation domain [42,43]. One possible effect of the RUNX2 p.Ala84-Ala89del would be enhanced activation of RUNX2 partners or downstream targets, consistent with the observed gain-of-function. The observed GOF effect could also be due to modification of the secondary and/or tertiary structure of the protein that could potentially affect the binding of RUNX2 or some of its isoforms to either the DNA of target genes or to cofactors/additional transcription factor. This could ultimately lead to increased expression of *RUNX2* or loss of its interaction with a repressor [44]. This deletion was previously found in 7 out of 160 alleles from unrelated unaffected individuals [45]. In our NCS cohort, we found a significant difference ($P = 2.83 \times 10^{-5}$) in the allele frequency of this deletion compared to the general population, 0.119 vs 0.0813, respectively. The difference in allele frequency was even more significant in our sNCS subtype cohort ($P = 1.28 \times 10^{-6}$), suggesting that role of this deletion in NCS may be subtype specific. Additionally, our data suggest that this deletion may possibly contribute to the etiology of NCS, based on the demonstrated GOF effect, although further functional experiments in animal models would be necessary to confirm this. Recently, Gustafson and colleagues identified a positive correlation between increased expression of *RUNX2* and insulin-like growth factor-1 (*IGF1*) in calvarial osteoblasts isolated from single suture CS patients [46]. They also demonstrated that cells with increased *IGF1* expression have decreased activity the GSK3β serine/threonine kinase, known to inhibit *RUNX2*. These observations enabled postulating a

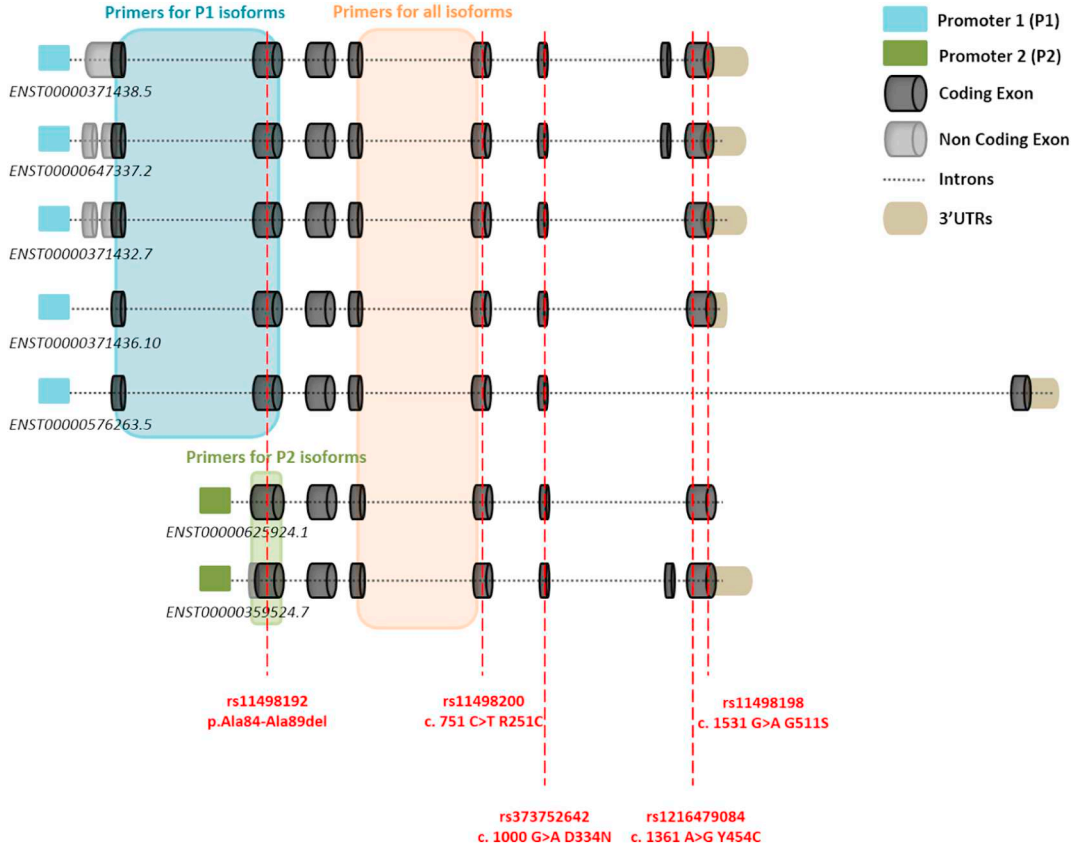

Fig. 1. *RUNX2* coding variants. The diagram shows the schematic structure of the 7 coding isoforms of *RUNX2* gene (source https://www.ensembl.org/; GRCh38), including the promoters, the coding and non-coding exons, the introns and the alternative untranslated regions at the 3′ end (3′UTRs). The large colored boxes span the regions amplified by the RT-qPCR primer sets (see Supplemental Table 1). The red dotted lines indicate the localization of 5 identified *RUNX2* mutations (see Table 1 and text for details). (For interpretation of the references to color in this figure legend, the reader is referred to the web version of this article.)

novel polygenic inheritance model for nonsyndromic CS, according to which the role of *RUNX2* in the pathogenesis of synostosis is reinforced in the presence of either *IGF1* overexpression or of *GSK3β* loss-of-function [46]. This hypothesis, tested in animal models, deserves further validation in NCS patients' cohorts.

Additionally, we noted that three of the coding variants identified in this study (namely, p.Ala84-Ala89del, R251C and D334N) showing GOF effects, map in regions shared by all the coding isoforms of the *RUNX2* gene, transcribed from both the distal (P1) and the proximal (P2) promoters. Park and collaborators previously demonstrated that the different RUNX2 transcripts bearing the two alternative promoters are involved in different stages of skull ossification [26]. Indeed, the proximal promoter P2 tends to be expressed during early in the primordial cartilage that is not destined to be mineralized, whereas the distal promoter P1 seemes to contribute to later skeletogenic events including osteoblast differentiation and maintenance, during calvarial morphogenesis [26]. We may thus speculate that the presence of these sequence variants would affect both early and late osteogenic events regulated by RUNX2 during skull morphogenesis.

Conversely, the Y454C and G511A variants map in an exon that is skipped in the ENST00000576263.5 isoform, deriving from the alternative splicing of the *RUNX2-P1* transcript (Fig. 1). Both these variants failed to show significant GOF effect in luciferase assay, therefore we cannot speculate further on their functional consequence with regard to

Table 1
RUNX2 variants in NCS. [a] Represents allele frequency in our cohort based on available exon coverage (*P* represents significance at a level of <0.05 compared to Global frequency); [b] Global frequency for non-Finnish European population based on GnomAD; * variants selected for functional analyses. p.Ala84-Ala89del was scored in both sNCS and mNCS and the rest of the variants were scored only in the sNCS cohort.

RUNX 2 Variant	*Allele Frequency* [a]	*SIFT Score*	*PPH score*	*Prediction*	*dbSNP*	*Global Frequency* [b]
p.Ala84-Ala89del*	84/540 sNCS ($P = 1.28 \times 10^{-6}$) 26/382mNCS ($P = 0.193$)	0.00	N/A	Probably damaging	rs11498192	7313/89912
c. 751C > T R251C*	1/430 sNCS ($P = 1 \times 10^{-5}$)	0.018	1	Damaging/probably damaging	rs11498200	4/113752
c. 1000 G > A D334N*	1/428 sNCS ($P = 1 \times 10^{-5}$)	0.003	0.943	Damaging/possibly damaging	rs373752642	1/113524
c. 1361 A > G Y454C	1/416 sNCS ($P = 1 \times 10^{-5}$)	0.00	1	Damaging/probably damaging	rs1216479084	1/113192
c. 1531 G > A G511S*	2/416 sNCS ($P = 0.215$)	0.07	1	Tolerated/probably damaging	rs11498198	1452/128818

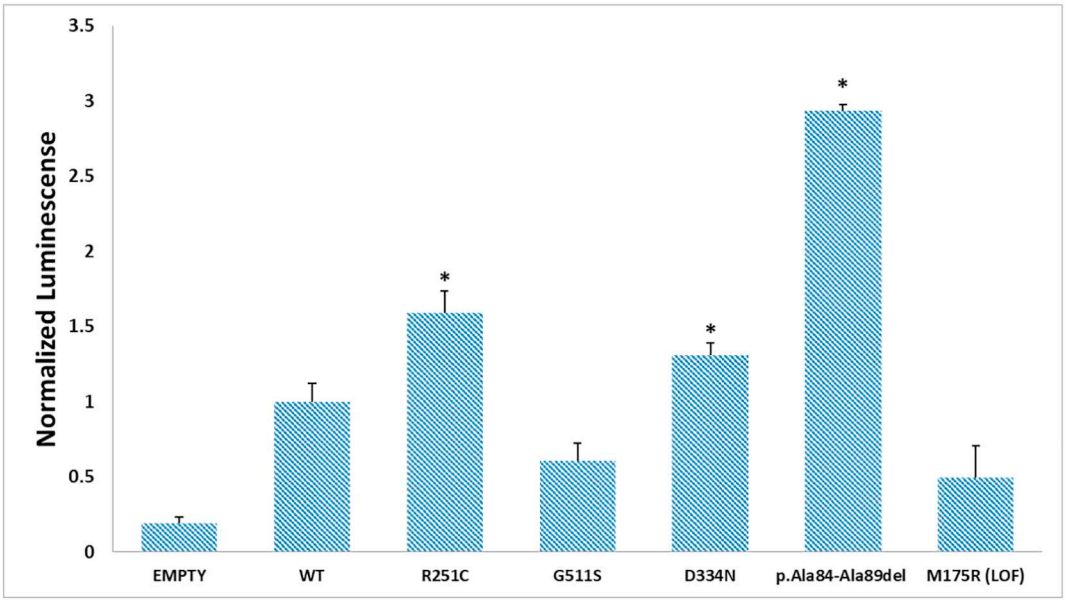

Fig. 2. Dual-luciferase assay of *RUNX2* variants. Control calvarial osteoblasts were transfected with (1) pOSE2-Luc reporter vector and (2) one of five *RUNX2* variants in a pCMV6 vector with minimal promoter. Transfection of pOSE2-Luc (OSE2 binding element) alone resulted in negligible luciferase production. Six independent replicates were tested for each construct. *Renilla* vectors were used as internal transfection controls for all experiments. (*) represents significance at a level of <0.05 compared to the wild-type (WT). Bars represent mean ± SE.

transcript isoforms.

Our data showed that the expression of *RUNX2* in suture tissues and CMSC of NCS patients is consistent with its role in the membranous ossification. Nonetheless, the expression data are inherently extremely heterogeneous, especially in the case of suture tissues analyzed. This shortcoming may be due to the inter-individual variability, the poor reproducibility of the precise collection sites during surgery, and the variable ages of patients at surgery, which ranged between 4 and 12 months (a crucial time frame of rapid growth of the postnatal brain and skull) [47]. We have previously demonstrated that the differences between fused/unfused suture-derived cells are reproducible across different suture sites. All CMSC indeed express the same mesenchymal-like phenotype, as assessed by cytometry [33]. Also, upon an *in vitro* induction, CMSC homogeneously overexpress osteogenic genes (*BMP2*, *Osteocalcin*, *RUNX2,* and *Osterix*) as a result of their osteogenic commitment and differentiation, regardless of the suture site they are isolated from [33]. Nonetheless, the differential expression of *RUNX2* isoforms in different suture sites, reflects the different chronology of suture fusion patterns, given the role of this master transcription factor. Our data are consistent with previous observations indicating that the transcript variants derived from the P1 promoter are specifically needed during bone formation and stimulated by the osteogenic process [26,27]. Total RUNX2 is downregulated in fused sutures of both sagittal and metopic NCS patients, compared with unfused sutures, indicating completion of the osteogenic process. We found significantly lower total RUNX2 and P1-isoform levels in fused metopic sutures than in fused sagittal suture tissues. This expression trend could reflect the different timing of ossification that characterizes the two different suture sites: the metopic suture completes ossification between 3 and 9 months of age, while complete ossification of the sagittal suture may occur very late in adult life [48]. P2 isoforms do not seem to be relevant in this process, consistent with the extant literature [26,27].

The observed gene expression trend in suture-derived CMSC provides additional insights into the role of *RUNX2* in balancing the proliferation/differentiation switch. We showed that cells isolated from fused metopic sutures, being reasonably more committed towards osteogenic differentiation, showed an increased expression of *RUNX2* over matched unfused suture derived cells. Cells from fused sagittal sutures exclusively overexpress the P1-transcribed isoforms compared with the unfused suture cells. No significant differences were found when comparing *RUNX2* expression levels between cells isolated from metopic and sagittal fused suture sites. These data suggest that, upon *ex vivo* isolation, skeletogenic mesenchymal stromal cells tend to display a similar phenotype and *RUNX2* expression pattern, regardless of the suture source. Interestingly, a previous study reported that the presence of the common Apert *FGFR2* p.P253R mutation is able to selectively regulate the alternative splicing of P1-isoforms, inducing the constitutive increase signaling of RUNX2 leading to excessive ossification [49].

5. Conclusions

In summary, our study suggests an etiopathogenetic role for *RUNX2* in the aberrant membranous ossification process occurring in at least a subset of individuals with midline NCS. Specifically, rare mutations of *RUNX2* with significant GOF effects could contribute to a proportion of midline NCS cases. Considering that the AF for RUNX2 p.Ala84-Ala89del was statistically different in sNCS versus the general population, it is plausible that its GOF effect is necessary and suture specific, but not sufficient for the development of CS. This deletion falls in a sequence region that is transcribed by both of the known alternative promoters of the gene. Recent data suggesting polygenic inheritance involving *RUNX2* increased function could be further tested as a novel etiological modality for nonsyndromic single suture CS [46]. Also, the expression data demonstrated that *RUNX2*, and particularly the P1-isoform group, are overexpressed in the osteogenic precursors within the pathological suture sites, which could lead to accelerated differentiation, resulting in premature fusion of the metopic and sagittal sutures. Further functional studies are needed to establish how the GOF variants affect the *RUNX2* isoform expression and/or DNA binding ultimately contributing to NCS.

Supplementary data to this article can be found online at https://doi.org/10.1016/j.bone.2020.115395.

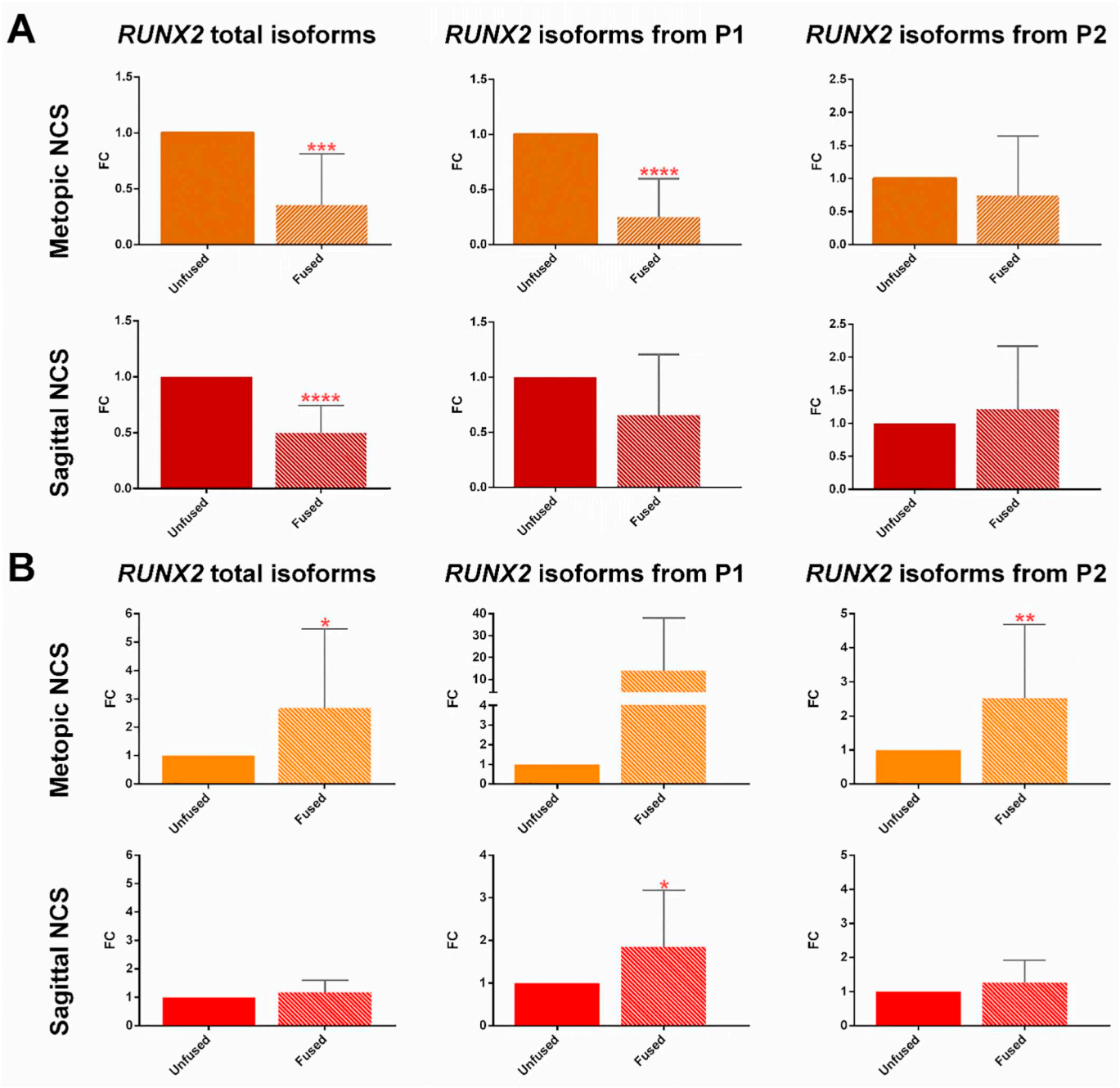

Fig. 3. *RUNX2* expression in mNCS and sNCS. The bar graphs show the relative expression of specific groups of *RUNX2* transcript isoforms (i.e. total, P1- and P2-derived isoforms) in patient-matched samples of both mNCS and sNCS (i.e. pairwise comparison between fused and unfused sutures from the same patient): A) expression levels analyzed in suture tissues; B) expression levels analyzed in suture-derived calvarial mesenchymal stromal cells (CMSC). *$P \leq 0.05$; **$P \leq 0.01$; ***$P \leq 0.001$; ****$P \leq 0.0001$.

Funding

This work was supported by the National Institutes of Health-NIDCR [grant number R01 DE-016886 to SB], Università Cattolica del Sacro Cuore ["linea-D1 2017-2018" intramural funds to WL] and by the "Federazione GENE" no-profit patient organization [research funds to WL].

CRediT authorship contribution statement

Araceli Cuellar: Conceptualization, Formal analysis, Writing - original draft.**Krithi Bala:**Conceptualization, Formal analysis, Writing - original draft.**Lorena Di Pietro:**Conceptualization, Formal analysis, Writing - original draft, Writing - review & editing.**Marta Barba:**Conceptualization, Formal analysis.**Garima Yagnik:** Conceptualization, Formal analysis.**Jia Lie Liu:**Project administration.**Christina Stevens:**Project administration.**David J. Hur:**Writing - review & editing.**Roxann G. Ingersoll:**Writing - review & editing.**Cristina M. Justice:**Formal analysis.**Hicham Drissi:**Writing - review & editing.**Jinoh Kim:**Writing - review & editing.**Wanda Lattanzi:**Conceptualization, Writing - original draft, Validation.**Simeon A. Boyadjiev:**Conceptualization, Formal analysis, Writing - original draft, Validation.

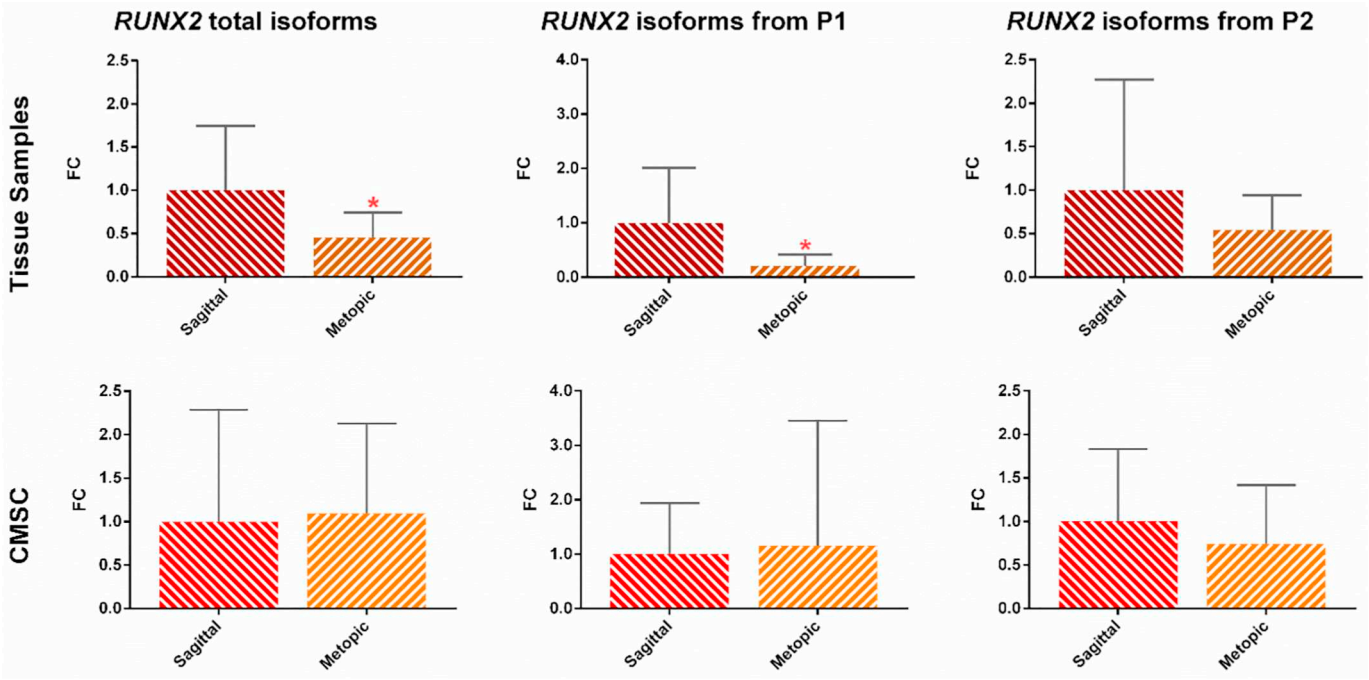

Fig. 4. *RUNX2* expression level comparison between different suture sites. The histograms show the expression levels of specific groups of *RUNX2* transcripts (i.e. total, P1- and P2-derived isoforms) in metopic and sagittal fused suture tissues and CMSC isolated thereof. $*P \leq 0.05$.

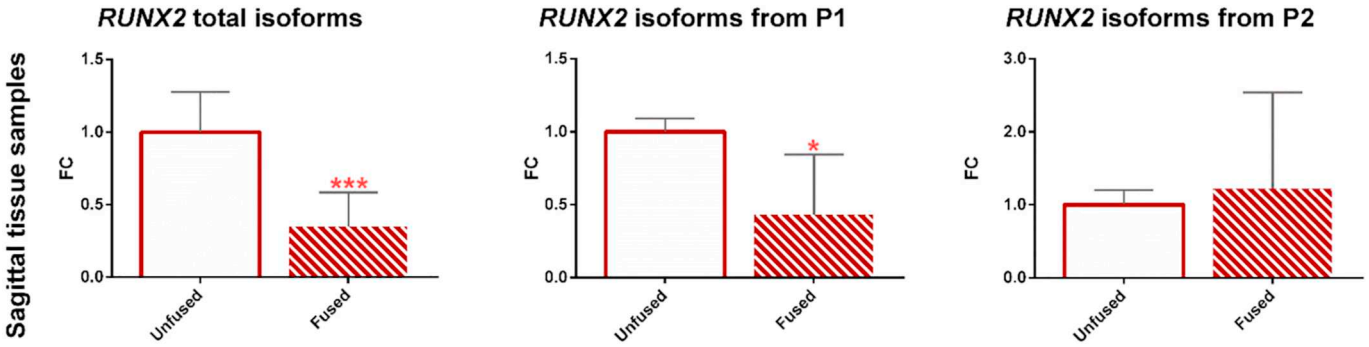

Fig. 5. *RUNX2* expression in unmatched sagittal tissue samples (i.e. fused and unfused samples from different individuals). The bar graphs display the expression levels of specific groups of *RUNX2* transcripts (i.e. total, P1- and P2-derived isoforms) in both fused and unfused sagittal suture tissues. $*P \leq 0.05$; $***P \leq 0.001$.

Declaration of competing interest

None.

Acknowledgements

We would like to thank all study participants for donating their time and providing the biological specimens to make this study possible. We thank Michael L Cunningham, Andrew OM Wilkie and Tony Roscioli for contributing samples to the sequencing cohort. We thank surgeons: Craig A. Vander Kolk, George Jallo, Jeffrey Marsh, Jayash Panchal, Craig Senders, Marike Zweinenberg, James Boggan, Gianpiero Tamburrini, Massimo Caldarelli, Luca Massimi and Paolo Frassanito for contributing bone samples and thank Enrico Guadagni, and Sarah Shandy for technical support.

References

[1] M.R. Passos-Bueno, A.L. Sertié, F.S. Jehee, R. Fanganiello, E. Yeh, Genetics of craniosynostosis: genes, syndromes, mutations and genotype-phenotype correlations, Front Oral Biol 12 (2008) 107–143, https://doi.org/10.1159/000115035.

[2] A.O. Wilkie, E.G. Bochukova, R.M. Hansen, I.B. Taylor, S.V. Rannan-Eliya, J.C. Byren, S.A. Wall, L. Ramos, M. Venâncio, J.A. Hurst, A.W. O'rourke, L.J. Williams, A. Seller, T. Lester, Clinical dividends from the molecular genetic diagnosis of craniosynostosis, Am. J. Med. Genet. A 143A (2007) 1941–1949, https://doi.org/10.1002/ajmg.a.31905.

[3] E.W. Jabs, Toward understanding the pathogenesis of craniosynostosis through clinical and molecular correlates, Clin. Genet. 53 (2008) 79–86, https://doi.org/10.1111/j.1399-0004.1998.tb02648.x.

[4] A.O.M. Wilkie, D. Johnson, S.A. Wall, Clinical genetics of craniosynostosis, Curr. Opin. Pediatr. 29 (2017) 622–628, https://doi.org/10.1097/MOP.0000000000000542.

[5] M. Poot, Structural genome variations related to craniosynostosis, Mol. Syndromol. 10 (2019) 24–39, https://doi.org/10.1159/000490480.

[6] S.R.F. Twigg, A.O.M. Wilkie, A genetic-pathophysiological framework for craniosynostosis, Am. J. Hum. Genet. 97 (2015) 359–377, https://doi.org/10.1016/j.ajhg.2015.07.006.

[7] Y. Heuzé, G. Holmes, I. Peter, J.T. Richtsmeier, E.W. Jabs, Closing the gap: genetic and genomic continuum from syndromic to nonsyndromic craniosynostoses, Curr. Genet. Med. Rep. 2 (2014) 135–145, https://doi.org/10.1007/s40142-014-0042-x.

[8] K.W. Gripp, D.M. McDonald-Mcginn, K. Gaudenz, L.A. Whitaker, S.P. Bartlett, P.M. Glat, L.B. Cassileth, R. Mayro, E.H. Zackai, M. Muenke, Identification of a genetic cause for isolated unilateral coronal synostosis: a unique mutation in the fibroblast growth factor receptor 3, J. Pediatr. 132 (1998) 714–716, https://doi.org/10.1016/S0022-3476(98)70366-X.

[9] J.B. Mulliken, K.W. Gripp, C.A. Stolle, D. Steinberger, U. Müller, Molecular analysis of patients with synostotic frontal plagiocephaly (unilateral coronal synostosis), Plast. Reconstr. Surg. 113 (2004) 1899–1909, https://doi.org/10.1097/01.PRS.0000122202.26792.BF.

[10] C.M. Seto, M.L. Hing, A.V. Chang, J. Hu, M. Kapp-Simon, K.A. Patel, P.K. Burton, B.K. Kane, A.A. Smyth, M.D. Hopper, R. Ellenbogen, R.G. Stevenson, K. Speltz, M.L. Cunningham, Isolated sagittal and coronal craniosynostosis associated with TWIST box mutations, Am. J. Med. Genet. A 143A (2007) 678–686, https://doi.org/10.1002/ajmg.a.31630.

[11] E. Lee, T. Le, Y. Zhu, G. Elakis, A. Turner, W. Lo, H. Venselaar, C.A. Verrenkamp, N. Snow, D. Mowat, E.P. Kirk, R. Sachdev, J. Smith, N.J. Brown, M. Wallis, C. Barnett, F. McKenzie, M.L. Freckmann, F. Collins, M. Chopra, N. Gregersen, I. Hayes, S. Rajagopalan, T.Y. Tan, Z. Stark, R. Savarirayan, A. Yeung, L. Adès, M. Gattas, K. Gibson, M. Gabbett, D.J. Amor, W. Lattanzi, S. Boyd, E. Haan, M. Gianoutsos, T.C. Cox, M.F. Buckley, T. Roscioli, A craniosynostosis massively parallel sequencing panel study in 309 Australian and New Zealand patients: findings and recommendations, Genet. Med. 20 (2018) 1061–1068, https://doi.org/10.1038/gim.2017.214.

[12] F. di Rocco, G. Baujat, E. Arnaud, D. Rénier, J.L. Laplanche, V.C. Daire, C. Collet, Clinical spectrum and outcomes in families with coronal synostosis and TCF12 mutations, Eur. J. Hum. Genet. 22 (2014) 1413–1416, https://doi.org/10.1038/ejhg.2014.57.

[13] W. Lattanzi, M. Barba, L. Di Pietro, S.A. Boyadjiev, Genetic advances in craniosynostosis, Am. J. Med. Genet. Part A. 173 (2017) 1406–1429, https://doi.org/10.1002/ajmg.a.38159.

[14] H.C. Mefford, N. Shafer, F. Antonacci, J.M. Tsai, S.S. Park, A.V. Hing, M.J. Rieder, M.D. Smyth, M.L. Speltz, E.E. Eichler, M.L. Cunningham, Copy number variation analysis in single-suture craniosynostosis: multiple rare variants including RUNX2 duplication in two cousins with metopic craniosynostosis, Am. J. Med. Genet. Part A. 152 (2010) 2203–2210, https://doi.org/10.1002/ajmg.a.33557.

[15] L.J. Williams, T. Lester, H.J. Beaumont, M. Crocker, C. Noakes, A. Stefanidou, C. Sarri, E. Bazopoulou-Kyrkanidou, A. Seller, M.B. Petersen, A.O.M. Wilkie, A novel case of craniosynostosis caused by a 6p21 duplication that includes the entire RUNX2 gene, J. Med. Genet. 42 (2005) S106.

[16] K. Varvagiannis, A. Stefanidou, Y. Gyftodimou, H. Lord, L. Williams, C. Sarri, E. Pandelia, E. Bazopoulou-Kyrkanidou, C. Noakes, T. Lester, A.O.M. Wilkie, M.B. Petersen, Pure de novo partial trisomy 6p in a girl with craniosynostosis, Am. J. Med. Genet. Part A. 161 (2013) 343–351, https://doi.org/10.1002/ajmg.a.35727.

[17] M.R. Greives, E.A. Odessey, D.J. Waggoner, D.S. Shenaq, S. Aradhya, A. Mitchell, E. Whitcomb, N. Warshawsky, T.C. He, R.R. Reid, RUNX2 quadruplication: additional evidence toward a new form of syndromic craniosynostosis, J Craniofac Surg 24 (2013) 126–129, https://doi.org/10.1097/SCS.0b013e31826686d3.

[18] A. Tessa, S. Salvi, C. Casali, L. Garavelli, M.C. Digilio, M.T. Dotti, S. Di Giandomenico, M. Valoppi, G.S. Grieco, G. Comanducci, G. Bianchini, D. Fortini, A. Federico, A. Giannotti, F.M. Santorelli, Six novel mutations of the RUNX2 gene in Italian patients with cleidocranial dysplasia, Hum. Mutat. 22 (2003) 104, https://doi.org/10.1002/humu.9155.

[19] P. Ducy, R. Zhang, V. Geoffroy, A.L. Ridall, G. Karsenty, Osf2/Cbfa1: a transcriptional activator of osteoblast differentiation, Cell 89 (1997) 747–754, https://doi.org/10.1016/S0092-8674(00)80257-3.

[20] F. Otto, A.P. Thornell, T. Crompton, A. Denzel, K.C. Gilmour, I.R. Rosewell, G.W.H. Stamp, R.S.P. Beddington, S. Mundlos, B.R. Olsen, P.B. Selby, M.J. Owen, Cbfa1, a candidate gene for cleidocranial dysplasia syndrome, is essential for osteoblast differentiation and bone development, Cell 89 (1997) 765–771, https://doi.org/10.1016/S0092-8674(00)80259-7.

[21] T. Komori, Regulation of bone development and extracellular matrix protein genes by RUNX2, Cell Tissue Res. 339 (2010) 189–195, https://doi.org/10.1007/s00441-009-0832-8.

[22] T. Komori, Roles of Runx2 in skeletal development, Adv. Exp. Med. Biol. 962 (2017) 83–93, https://doi.org/10.1007/978-981-10-3233-2_6.

[23] J.C. Liu, C.J. Lengner, T. Gaur, Y. Lou, S. Hussain, M.D. Jones, B. Borodic, J.L. Colby, H.A. Steinman, A.J. Van Wijnen, J.L. Stein, S.N. Jones, G.S. Stein, J.B. Lian, Runx2 protein expression utilizes the Runx2 P1 promoter to establish osteoprogenitor cell number for normal bone formation, J. Biol. Chem. 286 (2011) 30057–30070, https://doi.org/10.1074/jbc.M111.241505.

[24] M. Stock, F. Otto, Control of RUNX2 isoform expression: the role of promoters and enhancers, J. Cell. Biochem. 95 (2005) 506–517, https://doi.org/10.1002/jcb.20471.

[25] A. Takahashi, M.C. de Andrés, K. Hashimoto, E. Itoi, M. Otero, M.B. Goldring, R.O.C. Oreffo, DNA methylation of the RUNX2 P1 promoter mediates MMP13 transcription in chondrocytes, Sci. Rep. 7 (2017) 1–10, https://doi.org/10.1038/s41598-017-08418-8.

[26] M.H. Park, H.I. Shin, J.Y. Choi, S.H. Nam, Y.J. Kim, H.J. Kim, H.M. Ryoo, Differential expression patterns of Runx2 isoforms in cranial suture morphogenesis, J. Bone Miner. Res. 16 (2001) 885–892, https://doi.org/10.1359/jbmr.2001.16.5.885.

[27] H. Tamiya, T. Ikeda, J.H. Jeong, T. Saito, F. Yano, Y.K. Jung, S. Ohba, H. Kawaguchi, U.I. Chung, J.Y. Choi, Analysis of the Runx2 promoter in osseous and non-osseous cells and identification of HIF2A as a potent transcription activator, Gene 416 (2008) 53–60, https://doi.org/10.1016/j.gene.2008.03.003.

[28] K. Cartharius, K. Frech, K. Grote, B. Klocke, M. Haltmeier, A. Klingenhoff, M. Frisch, M. Bayerlein, T. Werner, MatInspector and beyond: promoter analysis based on transcription factor binding sites, Bioinformatics 21 (2005) 2933–2942, https://doi.org/10.1093/bioinformatics/bti473.

[29] J. Schug, Using TESS to predict transcription factor binding sites in DNA sequence, Curr Protoc Bioinformatics. Chapter 2 (2008), https://doi.org/10.1002/0471250953.bi0206s21.

[30] G.G. Loots, I. Ovcharenko, rVISTA 2.0: evolutionary analysis of transcription factor binding sites, Nucleic Acids Res. 32 (2004) 217–221, https://doi.org/10.1093/nar/gkh383.

[31] M.G. Reese, F.H. Eeckman, D. Kulp, D. Haussler, Improved splice site detection in Genie, J. Comput. Biol. 4 (1997) 311–323, https://doi.org/10.1089/cmb.1997.4.311.

[32] M. Barba, L. Di Pietro, L. Massimi, M.C. Geloso, P. Frassanito, M. Caldarelli, F. Michetti, S. Della Longa, P.A. Romitti, C. Di Rocco, A. Arcovito, O. Parolini, G. Tamburrini, C. Bernardini, S.A. Boyadjiev, W. Lattanzi, BBS9 gene in non-syndromic craniosynostosis: role of the primary cilium in the aberrant ossification of the suture osteogenic niche, Bone 112 (2018) 58–70, https://doi.org/10.1016/j.bone.2018.04.013.

[33] W. Lattanzi, M. Barba, F. Novegno, L. Massimi, V. Tesori, G. Tamburrini, S. Galgano, C. Bernardini, M. Caldarelli, F. Michetti, C. Di Rocco, Lim mineralization protein is involved in the premature calvarial ossification in sporadic craniosynostoses, Bone 52 (2013) 474–484, https://doi.org/10.1016/j.bone.2012.09.004.

[34] L. Tou, N. Quibria, J.M. Alexander, Transcriptional regulation of the human Runx2/Cbfa1 gene promoter by bone morphogenetic protein-7, Mol. Cell. Endocrinol. 205 (2003) 121–129, https://doi.org/10.1016/S0303-7207(03)00151-5.

[35] K.J. Livak, T.D. Schmittgen, Analysis of relative gene expression data using real-time quantitative PCR and the 2-ΔΔCT method, Methods 25 (2001) 402–408, https://doi.org/10.1006/meth.2001.1262.

[36] L. Zeng, J. Wei, N. Zhao, S. Sun, Y. Wang, H. Feng, A novel 18-bp in-frame deletion mutation in RUNX2 causes cleidocranial dysplasia, Arch. Oral Biol. 96 (2018) 243–248, https://doi.org/10.1016/j.archoralbio.2017.10.020.

[37] T. Schaap, The applicability of the Hardy-Weinberg principle in the study of populations, Ann. Hum. Genet. 44 (1980) 211–215, https://doi.org/10.1111/j.1469-1809.1980.tb00960.x.

[38] B. Lee, K. Thirunavukkarasu, L. Zhou, L. Pastore, A. Baldini, J. Hecht, V. Geoffroy, P. Ducy, G. Karsenty, Missense mutations abolishing DNA binding of the osteoblast-specific transcription factor OSF2/CBFA1 in cleidocranial dysplasia, Nat. Genet. 16 (1997) 307–310, https://doi.org/10.1038/ng0797-307 (PMID: 9207800).

[39] T. Takarada, R. Nakazato, A. Tsuchikane, K. Fujikawa, T. Iezaki, Y. Yoneda, E. Hinoi, Genetic analysis of Runx2 function during intramembranous ossification, Dev 143 (2016) 211–218, https://doi.org/10.1242/dev.128793.

[40] A. Molin, S. Lopez-Cazaux, O. Pichon, M. Vincent, B. Isidor, C. Le Caignec, Patients with isolated oligo/hypodontia caused by RUNX2 duplication, Am. J. Med. Genet. Part A. 167 (2015) 1386–1390, https://doi.org/10.1002/ajmg.a.37052.

[41] T. Maeno, T. Moriishi, C.A. Yoshida, H. Komori, N. Kanatani, S. Izumi, K. Takaoka, T. Komori, Early onset of Runx2 expression caused craniosynostosis, ectopic bone formation, and limb defects, Bone 49 (2011) 673–682, https://doi.org/10.1016/j.bone.2011.07.023 PMID: 21807129.

[42] S. Sato, A. Kimura, J. Ozdemir, Y. Asou, M. Miyazaki, T. Jinno, K. Ae, X. Liu, M. Osaki, Y. Takeuchi, S. Fukumoto, H. Kawaguchi, H. Haro, K.I. Shinomiya, G. Karsenty, S. Takeda, The distinct role of the runx proteins in chondrocyte differentiation and intervertebral disc degeneration: findings in murine models and in human disease, Arthritis Rheum. 58 (2008) 2764–2775, https://doi.org/10.1002/art.23805.

[43] K. Thirunavukkarasu, M. Mahajan, K.W. McLarren, S. Stifani, G. Karsenty, Two domains unique to osteoblast-specific transcription factor Osf2/Cbfa1 contribute to its transactivation function and its inability to heterodimerize with Cbfβ, Mol. Cell. Biol. 18 (1998) 4197–4208, https://doi.org/10.1128/mcb.18.7.4197.

[44] A. V. Postma, J.B.A. Van De Meerakker, I.B. Mathijssen, P. Barnett, V.M. Christoffels, A. Ilgun, J. Lam, A.A.M. Wilde, R.H.L. Deprez, A.F.M. Moorman, A gain-of-function TBX5 mutation is associated with atypical Holt-Oram syndrome and paroxysmal atrial fibrillation, Circ. Res. 102 (2008) 1433–1442. doi:https://doi.org/10.1161/CIRCRESAHA.107.168294.

[45] S. Mundlos, F. Otto, C. Mundlos, J.B. Mulliken, A.S. Aylsworth, S. Albright, D. Lindhout, W.G. Cole, W. Henn, J.H.M. Knoll, M.J. Owen, R. Mertelsmann, B.U. Zabel, B.R. Olsen, Mutations involving the transcription factor CBFA1 cause cleidocranial dysplasia, Cell 89 (1997) 773–779, https://doi.org/10.1016/S0092-8674(00)80260-3.

[46] J.A. Gustafson, S.S. Park, M.L. Cunningham, Calvarial osteoblast gene expression in patients with craniosynostosis leads to novel polygenic mouse model, PLoS One 14 (2019) 1–14, https://doi.org/10.1371/journal.pone.0221402.

[47] M.R. Proctor, J.G. Meara, A review of the management of single-suture craniosynostosis, past, present, and future, J. Neurosurg. Pediatr. 24 (2019) 622–631, https://doi.org/10.3171/2019.7.PEDS18585.

[48] H.L. Vu, J. Panchal, E.E. Parker, N.S. Levine, P. Francel, The timing of physiologic closure of the metopic suture: a review of 159 patients using reconstructed 3D CT scans of the craniofacial region, J Craniofac Surg 12 (2001) 527–532, https://doi.org/10.1097/00001665-200111000-00005.

[49] T. Baroni, P. Carinci, C. Lilli, C. Bellucci, M.C. Aisa, L. Scapoli, S. Volinia, F. Carinci, F. Pezzetti, M. Calvitti, A. Farina, C. Conte, M. Bodo, P253R fibroblast growth factor receptor-2 mutation induces RUNX2 transcript variants and calvarial osteoblast differentiation, J. Cell. Physiol. 202 (2005) 524–535, https://doi.org/10.1002/jcp.20148.